DENTAL MATERIALS XXX (XXXX) XXX–XXX

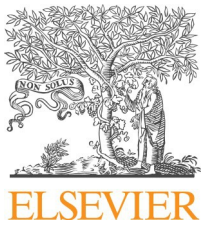

Available online at www.sciencedirect.com

ScienceDirect

journal homepage: www.elsevier.com/locate/dental

Determination of the spectrally resolved extinction coefficient of human dental enamel using collimated transmission spectroscopy

Karsten Pink[a,b,*], *Sascha Hein*[c], *Florian Foschum*[a], *Alwin Kienle*[a,b]

[a] *Institut für Lasertechnologien in der Medizin und Meßtechnik an der Universität Ulm, Helmholzstr. 12, 89081 Ulm, Germany*

[b] *Universität Ulm, Albert-Einstein-Allee 11, 89081 Ulm, Germany*

[c] *Emulation S. Hein, Rennweg 17, 79106 Freiburg im Breisgau, Germany*

ARTICLE INFO

Article history:
Received 18 March 2022
Received in revised form 22 August 2022
Accepted 29 August 2022

Keywords:
Extinction coefficient
Optical properties
Collimated transmission spectroscopy
Enamel
Optical appearance

ABSTRACT

Objectives: The determination of the extinction coefficient of human dental enamel to deliver further optical properties of enamel to improve the understanding of light propagation in teeth and to improve restoration materials.

Methods: The extinction coefficient was measured within a spectral range of 300–980 nm using a collimated transmission setup. 35 specimens from 16 donors were examined. The donors were categorized by age and the researched specimen were categorized by tooth type, tooth quality and lateral expansion of the enamel to clarify the influence of these parameters.

Results: The obtained spectrally resolved extinction coefficient was accurately described by a power law, which agrees with theoretical scattering models. The results were evaluated with regard to the influence of parameters such as subject age, tooth type, enamel sample quality and enamel width. For this purpose, both the average values of multiple measurements of a single sample in a defined spectral range as well as the curve slope of the averaged results versus wavelength were compared.

Significance: The results provide detailed information about the optical properties of human enamel. The wide spectrum investigated provides important information for the evaluation of the main scatterers and the optical impression under any light condition. However, the deviation of the extinction coefficient varies less between the mean values for the specimens grouped by several parameters than between the specimens themselves within a group. This indicates a unique optical behaviour for every specimen and this requires consideration in the development of artificial materials.

* Corresponding author at: Institut für Lasertechnologien in der Medizin und Meßtechnik an der Universität Ulm, Helmholzstr. 12, 89081 Ulm, Germany.
E-mail address: karsten.pink@ilm-ulm.de (K. Pink).

https://doi.org/10.1016/j.dental.2022.08.013
0109-5641/

1. Introduction

The optical appearance of human teeth has been of great interest especially in recent decades. Bright and uniformly looking teeth are seen as a standard of beauty and health [1]. This is especially important when it comes to the restoration and replacement of teeth [2]. For the development of restorative materials knowledge and accurate characterization of the tooth's optical behaviour is very important. To get natural-looking teeth, it is essential to understand the appearance of teeth in different surroundings and light conditions. Therefore, the description of the light propagation in teeth is of great interest and has been a relevant field of research [3,4]. For example, Zijp et al. showed that the angularly resolved reflectance from enamel probes at 3 specific wavelengths, 632.8 nm, 594.1 nm and 543.5 nm, provides information about the scattering behaviour of dental enamel [5]. Research regarding the light propagation in human teeth compared to nano-filled resin-based composite was carried out by Elgendy et al.[6]. The translucency as an indicator for opacity of teeth is researched [7], there often the enamel and dentin are not considered separately. Some investigations of human enamel compared to bovine specimen using specular reflectance ellipsometric measurements and integrating sphere measurements have also been performed showing that the scattering behaviour in the visible range is similar for human and bovine samples of enamel, but the absorption differs by a factor of up to three. No significant difference in refractive index was found [8,9]. The optical properties in the mid-infrared spectral range of dental enamel have also been the subject of research, especially to obtain information for investigations concerning ablation via lasers in dentistry [10]. As the anatomy and composition of the enamel structure determines the light scattering and absorption, their changes can be used as an indicator for pathological alterations [11,12]. To get a deeper understanding of the light propagation in human teeth several simulations based on different models have been performed, varying from models of whole teeth [13,14] to models of single slabs of dental hard tissue [15] or restoration materials under external stress or while curing [16,17]. In these papers, the aim is to investigate the interaction of light at a certain depth and the so caused thermal heating of the tissue [18]. All these simulations use optical parameters that are determined experimentally and are dependent on wavelength. To improve the quality of the simulations more information about optical parameters is necessary. The appearance of teeth can be predicted and simulated exactly if the optical properties are known in detail. This is important for restorative medicine and plays also a big role in the physics based rendering [19,20] showing photorealistic looking teeth for example in games and movies. Further, if the optical properties of restorative materials are similar to those of real teeth, both will look the same under all lighting conditions. To get a more comprehensive view of the optical properties of human dental enamel, the evaluation of human specimens is indicated. The extinction coefficient μ_t, being the sum of the scattering coefficient μ_s and absorption coefficient μ_a, is one important parameter of the enamel to determine the appearance of teeth and this was the subject of this investigation. To the best of our knowledge, this was the first time that a spectrally resolved collimated transmission setup was used for the VIS-NIR range, to examine human dental enamel. This measurement provides a direct method to determine μt for a large number of specimens and over a wide spectrum of electromagnetic radiation. Furthermore, this setup enables the measurement of spatially small sample volumes of enamel. This allows several measurements at different positions on one tooth slab, which can show differences in optical properties within the same tooth. The limiting factor for this system is the specimen thickness multiplied by the scattering coefficient. If the product gets too high, this would indicate that the vast major type of scattering is derived from multiple scattering and the results would not be reliable. Normally, the thickness of the sample cannot be chosen arbitrarily thin and the scattering coefficient is invariable for these kinds of solid specimens. The results of the measurements are evaluated considering several parameters of the analyzed specimen like donors' age at explantation, lateral enamel dimension, enamel thickness and tooth type which gives the opportunity for statistical evaluation and provides information about the connection between the extinction coefficient and the examined parameter. The large acquired spectrum and the detailed evaluation considering the specimen parameter offer new insights relative to previous research. The aim of the study was to obtain the optical properties of a variety of different specimens and to compare them against each other while taking the mentioned parameters into account.

2. Materials and methods

2.1. Setup

To measure the extinction coefficient a spectroscopic system evaluating the collimated transmission was established. In Fig. 1 on the left, a schematic of the measurement setup is shown. White light, from a halogen and deuterium arc lamp (TIDAS® S 700 - CCD UV/NIR 2098 light source, J&M Analytik AG, Esslingen, Germany), is coupled into the system by a 200 μ m fibre (F) in front of a 180 μ m pinhole. The divergent light propagates through a variable aperture (A) to determine the spot size on the sample and is collimated by an off-axis parabolic mirror (PM) with a focal length of 152.5 mm. The collimated light propagates through a cuvette holding the sample (C+S) in a liquid surrounding. The sample was fixed with external tweezers to a laboratory holder, centred in the cuvette and aligned parallel to the cuvette wall and perpendicular to the beam direction. The position of each sample was checked ensuring that the illumination was only penetrating the enamel of the tooth slabs. For these measurements, a NaCl 0.9% solution (Plastipur, Fresenius SE & Co. KGaA, 61352 Bad Homburg, Germany) was used to keep the teeth moisturized and to prevent the enamel from cracking. Additionally, it provides a closer index matching between tooth and surrounding compared to air as surrounding medium which reduces reflections at the surface. The spot size on the teeth was adjusted to 1 mm in diameter to ensure the propagating light is only interacting with the enamel.

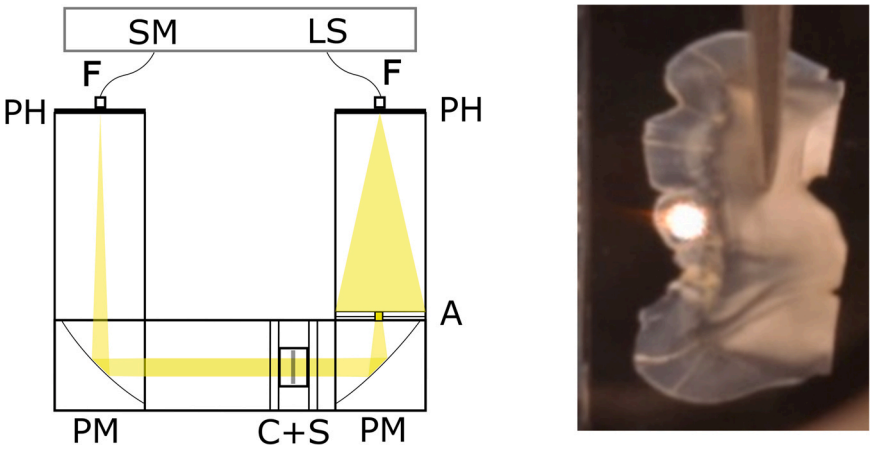

Fig. 1 – Left: Scheme of the measurement setup. Right: Slab of an investigated tooth with the illumination spot incident onto the enamel.

Pictures of the illuminating spot on the sample were taken to ensure and document the right positioning. One example can be seen in Fig. 1 on the right. The light behind the sample further propagates towards another off-axis parabolic mirror (PM) with the same focal length (152.5 mm). A pinhole with a diameter of 380 μ m is placed in the distance of the focal length of the parabolic mirror, directly followed by a fibre with a diameter of 660 μ m guiding the light towards a spectrometer (SM) (TIDAS® S 700 - CCD UV/NIR 2098, J&M Analytik AG, Esslingen, Germany). Due to the pinhole positioning in the Fourier plane of the parabolic mirror, the intensity of the angular distribution arriving at the parabolic mirror is translated into a spatially resolved intensity in the focal plane, which means that only light that is not absorbed and not scattered within a small solid angle $\theta_{\mathrm{lim}} = 0.00124$ rad around the forward direction will enter the detection fibre. Using the Henyey-Greenstein phase function [21] and an anisotropy factor $g = 0.96$ [22] or $g = 0.68$ [5] to determine the scattered light that is still detected, an error estimation of

$$\delta = \frac{\left(\frac{1}{2}\int_0^{\theta_{\mathrm{lim}}} \frac{1-g^2}{(1+g^2-2g\cos(\Theta))^{\frac{3}{2}}}\sin(\theta)\mathrm{d}\theta\right)(1-e^{-\bar{\mu_s}\bar{\mathrm{d}}})}{e^{-\bar{\mu_s}\bar{\mathrm{d}}}} \quad (1)$$

can be made, where $\bar{\mu_s} = 20\,\mathrm{mm}^{-1}$ and the sample thickness is $\bar{\mathrm{d}} = 0.2$ mm are assumed values in a plausible range. The denominator represents the probability that light is scattered and still detected. The numerator describes the probability that the light is not scattered and detected. For the described configuration the maximal estimated error for $g = 0.96$ is $\delta = 2.5\%$ and for $g = 0.68$ is $\delta = 0.034\%$. If the used phase function is modified by using an additional isotropic term as described by Friedl et al. [22], the error for $g = 0.96$ is reduced to $\delta = 1.65\%$ and for $g = 0.68$ to $\delta = 0.0236\%$. The approximation described by Eq. (1) is only valid if multiple scattering does not play a significant role.

The detection fibre can be shifted in two directions in the focal plane (x, y) to adjust the exact position for the best signal. This is necessary due to not perfectly plane parallel samples, which cause a shift in the position of the unscattered beam direction.

2.2. *Specimen*

This study was conducted on 35 tooth slices taken from 16 human teeth and covering every tooth type (lower and upper central and lateral incisors, canines, premolars and molars). This is a representative number of patients and the teeth were accessible. The age of the patients ranged from 10.4 to 67.25 years on the day of extraction. All teeth were extracted for orthodontic or periodontal reasons and supplied with consent forms, signed by each patient. Therefore the age distribution is not equal because orthodontic or periodontal issues occur less likely in the age group between 25 and 35. After cleaning and polishing with pumice, they were stored in a 0.1% thymol solution. Teeth with visually apparent discolourations, signs of caries or containing indirect restorations were excluded from the study. A water cooled slow speed saw (IsoMet LS, Buehler, Lake Bluff, IL, USA) was used together with a diamond disc for vertical slicing in a labio/bucco-lingual orientation. A grinder and polisher (EcoMet 250 Pro/AutoMet 250 Pro, Buehler, Lake Bluff, IL, USA) was used to reduce the thickness which was followed by fine grinding with wet 1200 and 2500 grit silicon carbide discs (Carbimet, Buehler, Lake Bluff, IL,USA). Measurements of the collimated transmission required both thin and highly polished ground sections. This was achieved with a polishing regime consisting of four cycles per surface, each lasting three minutes. Firstly, a synthetic silk cloth (VerduTex, Buehler, Lake Bluff, IL, USA) was used together with a diamond suspension containing 3 μm and 1 μm particles respectively. Lastly, a non-woven, pressed cloth (TexMet C, Buehler, Lake Bluff, IL, USA) was used with a diamond suspension of 0.25 μm and 0.05 μm particle size respectively. After completion, all samples were cleaned for 10 min in an ultrasonic bath with distilled water prior to measurements. The slabs had a thickness between 0.08 mm and 0.35 mm after preparation, measured using a micrometer. Each slab enamel was categorized according to

its lateral size using three categories. 'Narrow' describes enamel which only barely covers the illumination spot and only is present in some places of the specimen. 'Medium' describes enamel where the illumination spot fits in its dimensions easily on the enamel and 'wide' categorizes an enamel significantly larger in its lateral dimensions than the illumination area over the entire enamel.

2.3. *Measurement and evaluation*

The measurement is performed in three steps. First, a dark image is taken by blocking the illuminating, which gives the dark intensity I_{dark}. Then a reference measurement without a specimen in the filled cuvette is performed to get the reference intensity I_0 and finally the measurement of the sample is carried out which determines I_{sample}. Before the actual measurements the detection fibre is always adjusted to deliver the highest signal. Using the Lambert-Beer law [23,24].

$$I = I_0 e^{-\mu_t d} \tag{2}$$

and under consideration of the measurements mentioned above, Eq. (3) can be derived to determine the extinction coefficient

$$\mu_t = -\frac{1}{d}\ln\left(\frac{I_{sample} - I_{dark}}{I_0 - I_{dark}}\right). \tag{3}$$

μ_t can then directly be calculated considering the sample thickness d. All the measured intensities are spectrally dependent delivering the spectrally resolved extinction coefficient. Due to reflection at the specimen surface, caused by a refraction index mismatch, the equation needs to be modified to:

$$\mu_t = -\frac{1}{d}\ln\left(\frac{I_{sample} - I_{dark}}{I_0 - I_{dark}}\frac{1}{c_{tra}}\right), \tag{4}$$

where the transmission coefficient c_{tra}, based on the Fresnel reflection for perpendicular incidence at two successive interfaces neglecting multiple reflections [25], is introduced:

$$c_{tra} = \left(1 - \left(\frac{n_{enamel} - n_{NaCl}}{n_{enamel} + n_{NaCl}}\right)^2\right)^2. \tag{5}$$

The variables n_{enamel} and n_{NaCl} represent refractive indices of enamel and NaCl, respectively.

Each specimen was measured at five different locations on its enamel. This allows to study statistically the standard deviation of the measurements within the same sample. In order to compare the obtained curves with the theoretical models based on Mie scattering [26], a power law of the form

$$\mu_t(\lambda) = \mu_{t,0}\left(\frac{\lambda}{\lambda_0}\right)^{-b} \tag{6}$$

was fitted for each curve, as it is used for various human tissue scattering models [27,28], with $\lambda_0 = 600\,nm$.

3. Results

To get an overview of the large spectrum of results, mean values of the extinction coefficient for all samples are plotted in

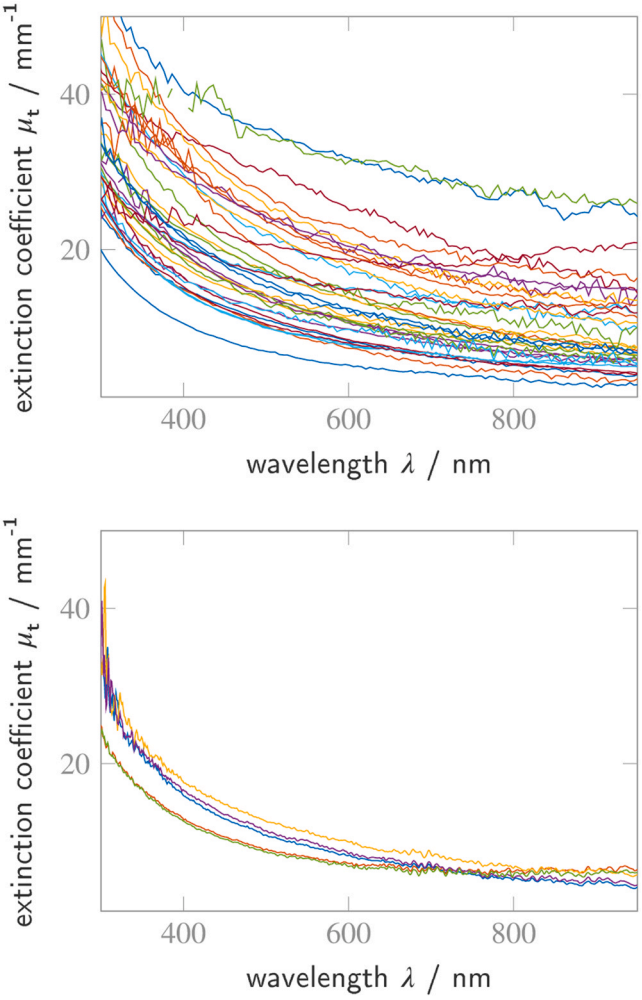

Fig. 2 – Top: mean extinction coefficient versus wavelength for the five measurements of all measured specimens. Bottom: Extinction coefficient versus wavelength for the five measured spots of one specimen.

Fig. 2 on the top. The curves show a large difference among each other, but they have similar behaviour versus wavelength. On the bottom an example of the measured curves of one specimen at five different spots is shown. The difference between these curves is much smaller and the characteristics are more similar compared to the curves of different samples.

In Fig. 3 the mean of the spectrally resolved extinction coefficient of the measured enamel samples is displayed. The standard deviation is extensive, as expected for biological probes. To outline the agreement of the measured data to the theory, a power law curve is fitted and also shown in Fig. 3. The curves differ only minimally demonstrating a good agreement between experiment and the power law. The coefficients for the power law are $\mu_{t,0} = 14.96 \pm 0.04\,mm^{-1}$ and $b = 1.149 \pm 0.06$ (with 95% confidence bounds).

Not least due to the large standard deviation of the extinction coefficient, for the different specimens, over the whole spectral range, the data were investigated considering the influence of different parameters. In Fig. 4 the extinction coefficient μ_t at a wavelength of 600 nm is shown for different

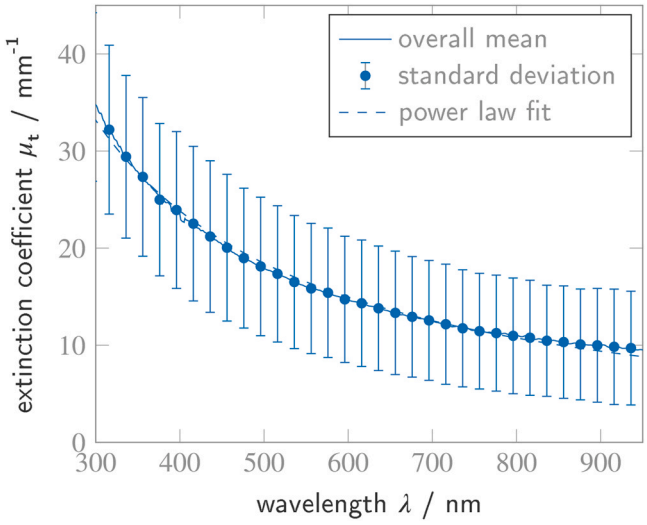

Fig. 3 – Mean value of the extinction coefficient of all measured specimens with standard deviation versus the measured spectral range and a fitted power law theory.

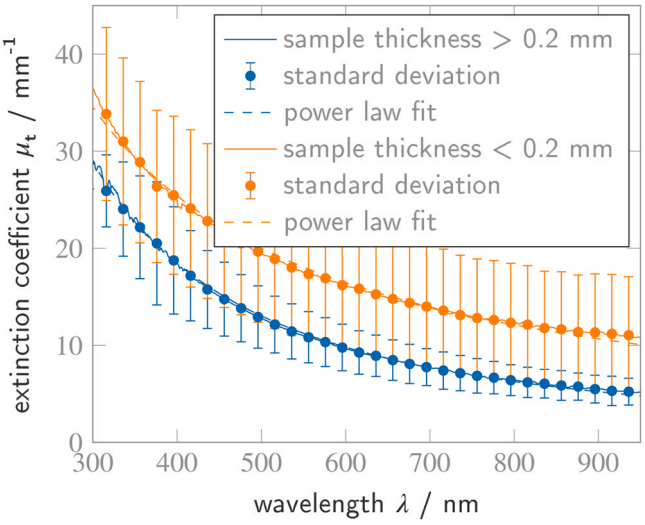

Fig. 5 – Extinction coefficient versus wavelength comparing the mean of the samples with a thickness over 0.2 mm and under 0.2 mm showing it's respective standard deviation.

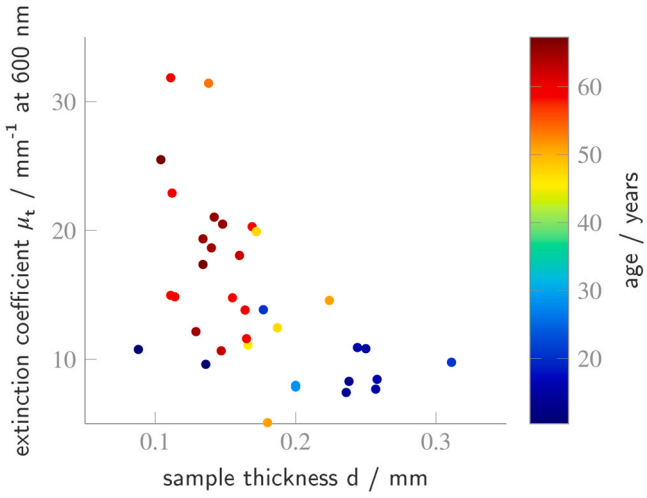

Fig. 4 – Extinction coefficient versus the sample thickness. The donors' age at explantation is coded by the colour of the data points.

thicknesses of the samples. In addition, the colour of the data points represents the donors' age at explantation. The thicker samples basically show a lower extinction coefficient but these samples are on average from donors of a younger age at explantation. For samples with a thickness between 0.08 mm and 0.2 mm the extinction coefficient varies over a range from 5.08 mm^{-1} to 31.85 mm^{-1}, whereas for samples with a thickness larger than 0.2 mm the extinction coefficient varies only between 7.42 mm^{-1} and 14.57 mm^{-1}. In general, surface scattering has a larger influence on thinner samples. It is also possible that aging causes the absorption to increase and the scattering to change what can cause an increase of the extinction coefficient dependent on which effect is prominent.

To illustrate the difference indicated by sample thickness, Fig. 5 shows the mean value of the extinction coefficient spectrally resolved and differentiated for specimens with a thickness larger than 0.2 mm and smaller than 0.2 mm. The difference can be seen over the whole spectrum and the standard deviation is smaller for the specimens thicker than 0.2 mm. A significant difference can also be seen in the coefficients of the power law fit, where for the specimens thinner than 0.2 mm $\mu_{t,0}$ = 16.460 ± 0.04 mm^{-1} and b = 1.069 ± 0.06 and for the specimens thicker than 0.2 mm $\mu_{t,0}$ = 9.811 ± 0.023 mm^{-1} and b = 1.556 ± 0.029 (with 95% confidence bounds).

The tooth type influences the thickness and shape of the enamel. To investigate if there is also an influence of the tooth type on the extinction coefficient, the extinction coefficient at 600 nm for all specimen, grouped by the tooth type, is shown in

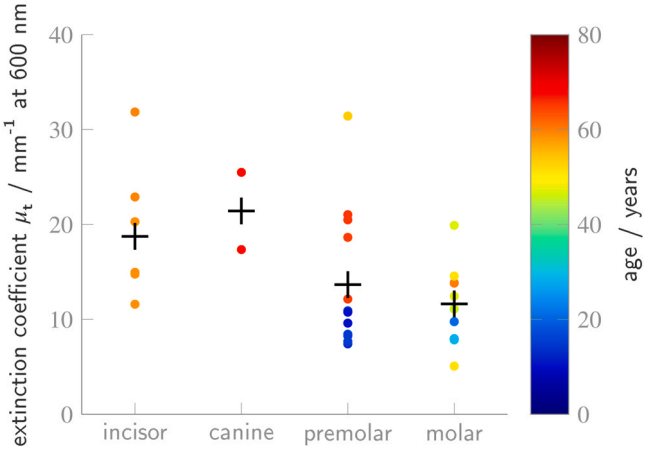

Fig. 6 – Extinction coefficient versus the different kinds of teeth. Donors' age at explantation is coded by the colour of the data points. The mean value of each group of teeth is represented by a vertical cross (+).

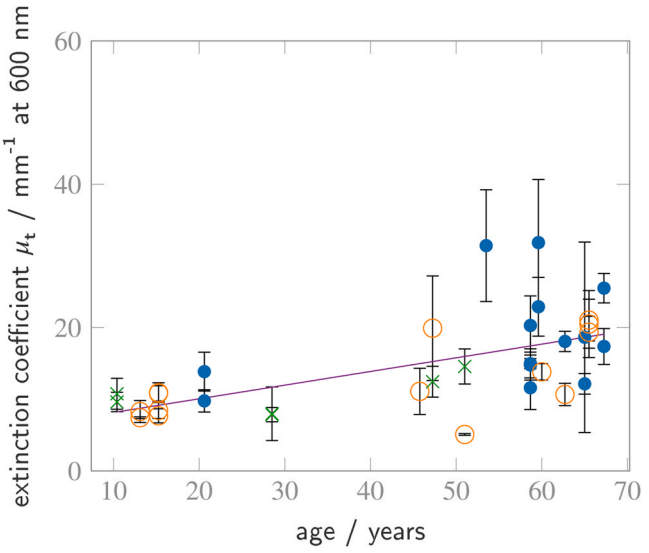

Fig. 7 – Extinction coefficient versus donors' age at explantation. The colour and shape of the mark represents the lateral size of the enamel. Blue dot(*)= 'narrow', orange circle(o) = 'medium', green cross(x) = 'wide'. The standard deviation and a regression line are shown as well.

Fig. 6. The average value of each tooth type, represented by the vertical cross, varies between 11.63 mm^{-1} and 21.43 mm^{-1}. Although the average value for incisors and canine specimen is higher than for premolar and molar teeth the difference in each group is higher than the differences of the average values respectively. Again, the colour coding shows the age distribution of the donors at explantation. According to these data the tooth type seems not to have a significant influence on the value of the extinction coefficient.

To determine whether the lateral size of the enamel influences the value of the extinction coefficient the teeth were, as mentioned above, categorized according to the lateral dimensions of the enamel. In Fig. 7 the extinction coefficient is plotted versus the donors' age at explantation, the colour and shape codes the lateral dimension of the enamel for each specimen. The regression line in this graphic shows a shows a positive slope between age and extinction coefficient. Taking the additional information about the lateral dimension of the enamel as well as the standard deviation into account this relation is not of a high significance. The green crosses representing laterally large enamel samples seem to have a lower extincion coefficient and a smaller standard deviation. This might be the case because less interaction of light at the enamels boundaries takes place.

Not only the absolute extinction coefficient for a specific wavelength, but also the behaviour of the extinction coefficient versus wavelength curve is of interest. In Fig. 8 the fit parameters $\mu_{t,0}$ and b versus the donors' age at explantation are shown. These values give information about the inclination and the overall height of the curve. The colour and shape of the data dots codes the tooth type. A regression line is given in Fig. 8 which shows an increase of $\mu_{t,0}$ with an increase of the donors age at explantation. The variation at a certain age is thereby larger than the difference between the age groups. The parameter b, which describes the curve slope, shows a decrease with the age of the donor at explantation. A regression line in Fig. 8 on the right shows this behaviour.

4. Discussion

The aim of this study was to determine the extinction coefficient of a heterogeneous group of human dental enamel samples and to evaluate the results, regarding the influences of several parameters like age or tooth type. The data found can be used for the calculation of light propagation for a variety of diagnostic and therapeutic applications and for the fabrication of dental restorative materials as well as for

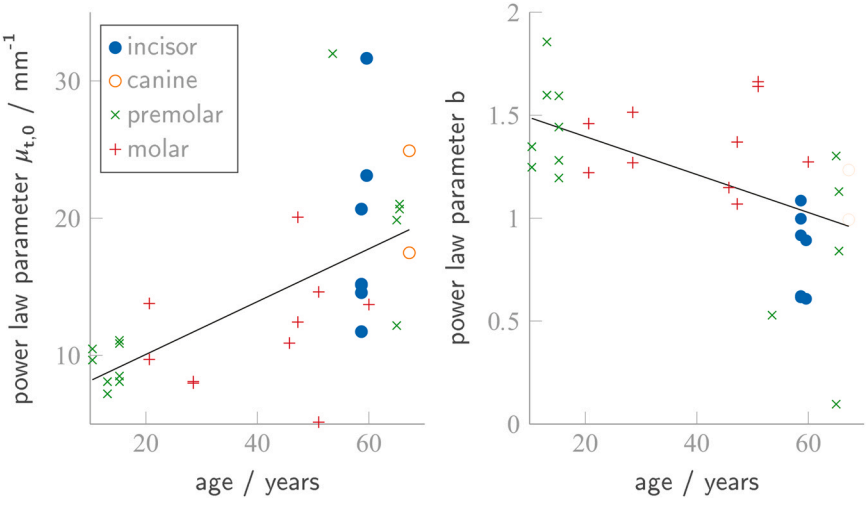

Fig. 8 – Left: power law parameter $\mu_{t,0}$ versus donors' age at explantation. Right: parameter b of the power law versus donors' age at explantation. The colour and shape represents the tooth type. Blue dot(*): incisor, orange circle(o): canine, green cross (x): premolar, red vertical cross(+): molar.

rendering applications. Several tendencies are shown in Section 3. A proportionality between age and extinction coefficient is shown. The tendency shows that the older the donor at explantation the higher the extinction coefficient. This is in contrast to the expectation that due to demineralization the scattering decreases over age. A reason for that behaviour can be an increase in absorption or an increase in scattering due to defects. A link between the fit parameters $\mu_{t,0}$ and b with the donors' age at explantation is also recognizable.These parameters indicate the change of the extinction coefficient versus wavelength. For older donors the value $\mu_{t,0}$ is higher but the parameter b which represents the decrease versus wavelength is lower. This indicates that in younger teeth the extinction coefficient shows a larger change and a steeper slope. However, the correlation is small compared to the standard deviation. An inverse proportionality between sample thickness and the extinction coefficient is presented, indicating a lower extinction coefficient for thicker probes. The non perfect surfaces of the samples and the so caused surface scattering can be the cause for that. The thinner the sample the larger is the impact of surface scattering on the total scattering. The standard deviation within every grouping of the results regarding a specific parameter was always more significant than the dependency between a parameter and the extinction coefficient. The measurement of the large number of different specimens shows a large variety of the extinction coefficient and indicates a rather unique appearance of the teeth. The extinction coefficient of the enamel does not show a clear dependency on the tooth type. However, this work was only a first step, further measurements like spectrally resolved goniometer experiments, integrating sphere measurements and reflectance measurements have to follow to obtain the whole optical data set. To further improve the understanding, the simulations based on the anatomy and the measured optical properties of light propagation in teeth should be extended and intensified [14]. We note that for this task also the anisotropic light propagation due to the aligned microstructure of enamel and dentin has to be considered [29–31].

5. Conclusion

This study was able to provide further information about the optical properties of human dental enamel. It could demonstrate that the optical properties vary substantially more between different donors than between various parameters such as age or tooth type. Therefore, the choice of a restorative material to replace human enamel, should be guided by the individual evaluation of the enamel of the neighbouring teeth, instead of following a formular that is based on overall shade prescription.

Data availability

Data underlying the results presented in this paper are not publicly available at this time but may be obtained from the authors upon reasonable request.

Disclosure

The authors declare no conflicts of interest.

REFERENCES

[1] Davis L, Ashworth P, Spriggs L. Psychological effects of aesthetic dental treatment. J Dent 1998;26(7):547–54.
[2] Dos Santos DM, Moreno A, Vechiato-Filho AJ, Bonatto LdR, Psqueira AA, Laurindo Júnior MCB, et al. The importance of the lifelike esthetic appearance of all-ceramic restorations on anterior teeth. Case Rep Dent 2015;2015.
[3] Zijp J, TenBosch J. Angular dependence of HeNe-laser light scattering by bovine and human dentine. Arch Oral Biol 1991;36(4):283–9.
[4] Zijp J.R. and tenBosch J.J. Two-dimensional patterns of Fraunhofer diffraction by dental enamel, 1995. 10.1117/12.228655.
[5] Zijp J, TenBosch J, Groenhuis R. HeNe-laser light scattering by human dental enamel. J Dent Res 1995;74(12):1891–8.
[6] Elgendy H, Maia RR, Skiff F, Denehy G, Qian F. Comparison of light propagation in dental tissues and nano-filled resin-based composite. Clin Oral Investig 2019;23:423–33. https://doi.org/10.1007/s00784-018-2451-9
[7] Lee YK. Translucency of human teeth and dental restorative materials and its clinical relevance. J Biomed Opt 2015;20(4):045002.
[8] Spitzer D, TenBosch J. The absorption and scattering of light in bovine and human dental enamel. Calcif Tissue Res 1975;17(2):129–37.
[9] Spitzer D, Ten JB. The total luminescence of bovine and human dental enamel. Calcif Tissue Res 1976;20(1):201–8.
[10] Zuerlein MJ, Fried D, Featherstone JD, Seka W. Optical properties of dental enamel in the mid-IR determined by pulsed photothermal radiometry. IEEE J Sel Top Quantum Electron 1999;5(4):1083–9.
[11] Hariri I, Sadr A, Shimada Y, Tagami J, Sumi Y. Effects of structural orientation of enamel and dentine on light attenuation and local refractive index: an optical coherence tomography study. J Dent 2012;40(5):387–96.
[12] Vaarkamp J, TenBosch J, Verdonschot E. Propagation of light through human dental enamel and dentine. Caries Res 1995;29(1):8–13.
[13] Fu Y, Jacques SL. Monte Carlo simulation for light propagation in 3D tooth model. Optical Interactions with Tissue and Cells XXII, volume 7897. SPIE,; 2022. p. 339–44.
[14] Zoller CJ, Hohmann A, Forschum F, Geiger S, Geiger M, Ertl TP, et al. Parallelized Monte Carlo software to efficiently simulate the light propagation in arbitrarily shaped objects and aligned scattering media. J Biomed Opt 2018;23(6):065004.
[15] Riva R, Watanuki JT, Myakawa W, Zezell DM, et al. Monte Carlo modelling of light propagation in hard dental tissues. Ann Opt 2004.
[16] Jerman E, Lümkemann N, Eichberger M, Zoller C, Nothelfer S, Kienle A, et al. Evaluation of translucency, Marten's hardness, biaxial flexural strength and fracture toughness of 3Y-TZP, 4Y-TZP and 5Y-TZP materials. Dent Mater 2021;37(2):212–22.
[17] Xie H, Basu S, DeMeter EC. Coupling Monte Carlo light propagation method and curing kinetic equations to model the degree of conversion evolution of UV-curable composites. Ind Eng Chem Res 2021;60(28):10431–44.

[18] Seka W, Fried D, Featherstone J, Borzillary S. Light deposition in dental hard tissue and simulated thermal response. J Dent Res 1995;74(4):1086–92.
[19] Shetty S. and Bailey M. A physical rendering model for human teeth.In ACM SIGGRAPH 2010 Posters, 2010: pp. 1–1.
[20] Jung J.W., Meyer G., DeLong R. and Holmes B.N. Rendering of human teeth and restorative biomaterials.In Color and Imaging Conference. 1, Society for Imaging Science and Technology, pp.170–176.
[21] Henyey LG, Greenstein JL. Diffuse radiation in the galaxy. Astrophys J 1941;93:70–83.
[22] Fried D, Glena RE, Featherstone JD, Seka W. Nature of light scattering in dental enamel and dentin at visible and near-infrared wavelengths. Appl Opt 1995;34(7):1278–85.
[23] Beer A. Bestimmung der Absorption des rothen Lichts in farbigen Flussigkeiten. Ann Phys 1852;162:78–88.
[24] Lambert J. Photometria sive de mensura et gradibus luminis colorum et umbrae augsburg.Detleffsen for the widow of Eberhard Klett 1760.
[25] Bohren CF, Huffman DR. Absorption and Scattering of Light by Small Particles. John Wiley & Sons; 2008.
[26] Mie G. Beiträge zur Optik trüber Medien, speziell kolloidaler Metallösungen. Ann der Phys 1908;330(3):377–445.
[27] Bashkatov AN, Genina E, Kochubey V, Tuchin V. Optical properties of human skin, subcutaneous and mucous tissues in the wavelength range from 400 to 2000 nm. J Phys D: Appl Phys 2005;38(15):2543.
[28] Jonasson H, Fredriksson I, Bergstrand S, Östgren CJ, Larsson M, Strömberg T. In vivo characterization of light scattering properties of human skin in the 475-to 850-nm wavelength range in a swedish cohort. J Biomed Opt 2018;23(12):121608.
[29] Kienle A, Forster FK, Diebolder R, Hibst R. Light propagation in dentin: influence of microstructure on anisotropy. Phys Med Biol 2003;48:N7–14. https://doi.org/10.1088/0031-9155/48/2/401
[30] Kienle A, Michels R, Hibst R. Magnification: a new look at a long-known optical property of dentin. J Dent Res 2006;85:955–9. https://doi.org/10.1177/154405910608501017
[31] Kienle A, Hibst R. Light Guiding in Biological tissue due to Scattering. Phys Rev Lett 2006;97(18104). https://doi.org/10.1103/physrevlett.97.018104